DOI: 10.1002/ejic.201100468

Regiospecific C(naphthyl)–H Bond Activation by Platinum(II) – Isolation, Characterization, Reactivity and TD-DFT Study of the Cycloplatinate Complexes

Achintesh Narayan Biswas,[a] Purak Das,[a] Vivek Bagchi,[b] Amitava Choudhury,[c] and Pinaki Bandyopadhyay*[a]

Keywords: C–H activation / Cyclometallation / Platinum / Oxidation / Density functional calculations

The regiospecific activation of C(naphthyl)–H bonds in a group of naphthylazo-2′-hydroxyarene ligands (H_2L) has been achieved by platinum(II) compounds under different reaction conditions, and stable cycloplatinates [$Pt^{II}L(D)$] have been isolated in presence of neutral Lewis bases (D). Structures of the cycloplatinate complexes of platinum(II) have been established by single-crystal X-ray crystallography. The platinum(II) centres are surrounded by a C,N,O-terdentate ligand frame (L) and Lewis base (D) in a distorted square planar fashion. These cycloplatinate species have been found to react with halogens and methyl iodide undergoing metal-centered two electron oxidation affording platinum(IV) cycloplatinates with distorted octahedral geometry. In the reactions with halogens and methyl iodide, *trans* oxidative addition has been found for [Pt(L)D] (D = 4-picoline), whereas *cis* addition has been observed for [Pt(L)D] where D is a more sterically demanding triphenylphosphane. Structures of two representative platinum(IV) cycloplatinate species have been determined by single-crystal X-ray crystallography. A time dependent (TD)-DFT study of representative cycloplatinate compounds has been performed. Optical absorption spectra of the cycloplatinate compounds in dichloromethane have been simulated using the TD-DFT method, and the experimental spectra are in very good agreement.

Introduction

Cyclometallation reactions are of considerable interest because of their role in the selective functionalization of C–H bonds[1] and numerous applications of the complexes derived.[2] The topic of C–H bond activation reactions promoted by platinum(II) complexes, as a key step in the functionalization of small molecules,[3] has undergone a rapid growth. Some representative examples where platinum(II) complexes have been extensively used includes alkane[3,4] and arene[5] functionalization, studies of their thermodynamic properties,[6] synthesis of complexes with interesting optical properties (luminescence),[7] C–C coupling reactions,[2c,8] metallomesogen chemistry[9] and anticancer agents.[10] Since the first report of platinum(II) organometallics containing a Pt–C(aryl) bond,[11] the study of cycloplatination reactions has mainly been confined to the domain of C(phenyl)–H bond activation.[9,12] Reports on C(naphthyl)–H bond activation by platinum(II) are relatively few.[13] Moreover, the low electrophilicity of platinum has been found to facilitate the stabilization of higher oxidation states, which is reflected in their ability to undergo oxidative addition reactions. A number of studies on oxidative addition reaction of platinum(II) compounds having monodentate and bidentate phosphorus or nitrogen ligands have been reported.[14–17] However, cycloplatinate compounds have not enjoyed the same popularity.[12e,16,18]

This work stems from our interest in the selective activation of different C(naphthyl)–H bonds by transition metal complexes.[19] Herein, selective C(naphthyl)–H bond

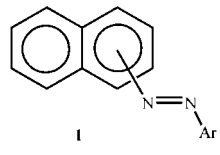

I

	Position of diazene (-N=N-)	Ar
H_2L^1	C-1	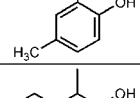
H_2L^2	C-1	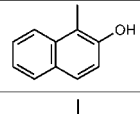
H_2L^3	C-2	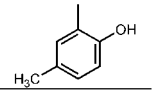

Scheme 1. Diazene ligands H_2L^1–H_2L^3.

[a] Department of Chemistry, University of North Bengal, Raja Rammohunpur,
Siliguri 734013, West Bengal, India
Fax: +91-353-2699001
E-mail: pbchem@rediffmail.com
[b] Department of Chemistry, Indian Institute of Technology, New Delhi 110016, India
[c] Department of Chemistry, Missouri S & T, Rolla, MO 65409, USA

Supporting information for this article is available on the WWW under http://dx.doi.org/10.1002/ejic.201100468.

activation by platinum(II) using a group of naphthylazo-2′-hydroxyarene ligands H_2L^1–H_2L^3 as substrates has been studied. The isolation and characterization of the resulting cycloplatinate species and rationalization of their structural and spectroscopic properties are described. Oxidative addition reactions of square planar divalent cycloplatinate compounds with halogens and methyl iodide are also reported. Moreover, a TD-DFT study of representative cycloplatinate species is presented (Scheme 1).

Results and Discussion

Cycloplatination Reactions

Ligands H_2L^1–H_2L^3 show a strong dependence on the platinum precursor and reaction conditions. Attempts to activate C(naphthyl)–H bonds using $K_2[PtCl_4]$ as the starting metal complex in ethanol met with failure. Subsequently, it was found that the diazene substrates H_2L^1–H_2L^3 react with the allyl platinum(II) complex $[(\eta^3\text{-}C_4H_7)\text{-}Pt(\mu\text{-}Cl)]_2$ in the presence of neutral Lewis bases (D) in chloroform to afford green monomeric cycloplatinate complexes **2**–**4** at room temperature. Only one cycloplatinate compound was obtained in each case. Cycloplatinate species **2**–**4** were isolated in their pure forms by preparative TLC in good yields (ca. 65%). Alternatively, the C(naphthyl)–H bond activation by $[(\eta^3\text{-}C_4H_7)Pt(\mu\text{-}Cl)]_2$ was also achieved on a solid surface. Cycloplatinate species were obtained in better yields (ca. 70–75%) by heating the reaction mixture adsorbed on silica gel at 120 °C for 6 h. The elemental analytical results and ^{1}H NMR spectroscopic data of **2**–**4** were consistent with their formulations as [Pt^{II}-(L)(D)]. The naphthyl group with the donor bearing substituents at C1 (H_2L^1 and H_2L^2) can offer C2–H or C8–H for metallation, whereas C1–H and C3–H are the potential metallation sites when the primary donor is attached to C2. X-ray crystallographic analyses of the representative cycloplatinates have been performed in order to ascertain their exact molecular structures.

Molecular structures of the divalent cyclometallates (**2a** and **2b**) derived from the reaction of H_2L^1 and $[(\eta^3\text{-}C_4H_7)\text{-}Pt(\mu\text{-}Cl)]_2$ are shown in Figures 1 and 2, respectively. The structures show monomeric compounds in which Pt is located in a slightly distorted square-planar environment, surrounded by the metallated C(2), N2 of the diazo group and O1 of the phenolato group of the dianionic terdentate ligand, and the fourth coordination site is occupied by N3 (**2a**) or P1 (**2b**) of the neutral donor molecule. The maximum deviations represented by the bite angles C(2)–Pt(1)–N(3) (**2a**) and C(2)–Pt(1)–P(1) (**2b**) are 100.9(2)° and 100.10(14)°, respectively. The Pt–N(azo) bond length [1.931(5) Å] is shorter than Pt–N(picoline) [2.035(6) Å] in **2a**, presumably due to the greater π-acceptor ability of the azo chromophore over the picoline moiety.[17] As a consequence, the N(1)–N(2) length of the coordinated azo group is elongated to 1.271(7) Å.

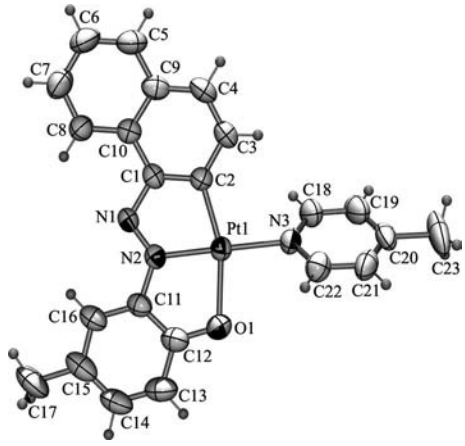

Figure 1. The asymmetric unit of **2a** with displacement ellipsoids drawn at 50% probability. Selected bond lengths [Å] and angles [°]: Pt1–C2 1.983(5), Pt1–N2 1.931(5), Pt1–O1 2.141(4), Pt1–N3 2.035(6), N1–N2 1.271(7), N1–C1 1.399(8), N2–C11 1.400(8), C2–Pt1–N3 100.9(2), N2–Pt1–O1 81.48(19), N2–Pt1–C2 79.5(2), N3–Pt1–O1 98.17(19).

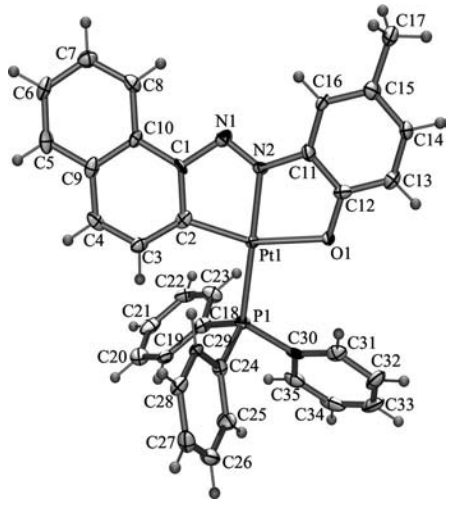

Figure 2. The asymmetric unit of **2b** with displacement ellipsoids drawn at 50% probability. Selected bond lengths [Å] and angles [°]: Pt1–C2 2.004(5), Pt1–N2 1.997(4), Pt1–O1 2.109(3), Pt1–P1 2.2543(12), N1–N2 1.275(5), N1–C1 1.406(6), N2–C11, 1.390(6), C2–Pt1–P1 100.10(14), N2–Pt1–O1 80.92(13), N2–Pt1– C2 79.04(17), P1–Pt1–O1 99.93(8).

Thus, regiospecific cycloplatination has been found to occur at the C2(naphthyl)–H bond of H_2L^1 in contrast to the exclusive C8(naphthyl)–H bond activation of H_2L^1 in the corresponding cyclopalladation reaction.[19]

Regiospecific C2(naphthyl)–H bond activation has also been observed in H_2L^2. The molecular geometry of **3a** is presented in Figure 3 with the atom numbering scheme. The platinum(II) centre in **3a** is bound to C2(naphthyl) of the 1-azonaphthyl fragment, N2 of the diazene group, O1 of the naphtholato group and N3 of picoline.

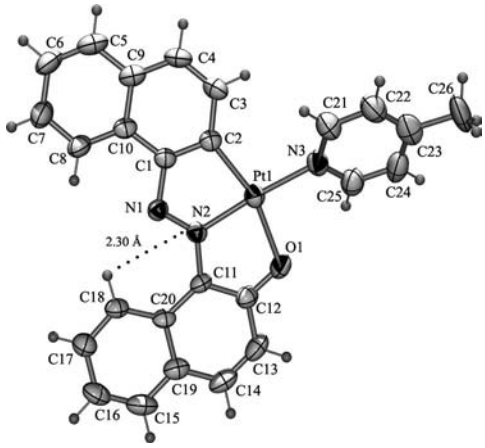

Figure 3. The asymmetric unit of **3a** with displacement ellipsoids drawn at 50% probability. Selected bond lengths [Å] and angles [°]: Pt1–C2 1.980(5), Pt1–N2 1.941(4), Pt1–O1 2.105(4), Pt1–N3 2.031(5), N1–N2 1.291(6), N1–C1 1.413(6), N2–C11 1.400(6), C2–Pt1–N3 103.41(19), N2–Pt1–O1 81.39(16), N2–Pt1–C2 80.27(18), N3–Pt1–O1 95.28(17).

The presence of the primary donor at C1 of the naphthalene rings in H_2L^1 and H_2L^2 results in regiospecific activation of the C(2)–H bond by platinum(II) irrespective of the nature of auxiliary donors (phenolato or naphtholato). The exclusive C2(naphthyl)–H bond activation can be rationalized as shown in Scheme 2. It is well known that cyclometalation is initiated through the coordination of the heteroatom to the metal centre. Subsequently the activation of C(naphthyl)–H bonds is governed by the formation of either five-membered carboplatinacycle or six-membered N,O chelate rings (Scheme 2). The formation of a carboplatinacycle ring results in the activation of the C2–H bond (route i, Scheme 1), whereas initial N,O chelation could lead to C8–H bond activation (route ii, Scheme 1). The reluctance of soft platinum(II) to bind hard phenolato/naphtholato donors in the initial stage excludes the possibility of C8(naphthyl)–H bond activation.

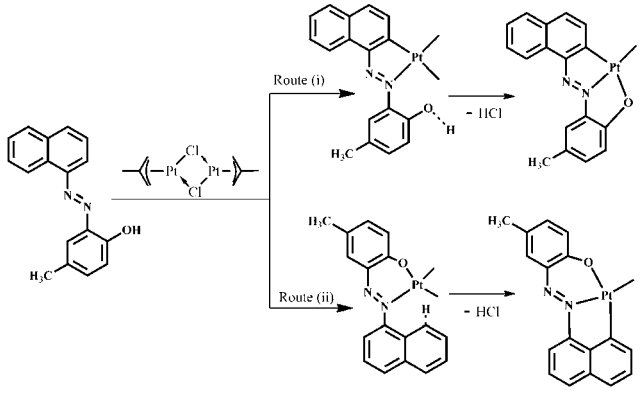

Scheme 2. Proposed sequential steps for activation of C2(naphthyl)–H, Route (i), and C8(naphthyl)–H, Route (ii).

The presence of the primary diazene group at C2 in H_2L^3 brings an additional factor into consideration. Here, C1(naphthyl)–H and C3(naphthyl)–H bonds are available for activation by platinum(II). Structure determination of **4a** (Figure 4), obtained from the reaction of H_2L^3 with $[(\eta^3\text{-}C_4H_7)Pt(\mu\text{-}Cl)]_2$ in the presence of 4-picoline, shows that the regiospecific activation of the C3(naphthyl)–H bond has occurred. The preferential activation of the C3(naphthyl)–H bond over the C1(naphthyl)–H bond of H_2L^3 by platinum(II) calls for an explanation. Attempts have been made to explain it in terms of the SHAB principle. DFT calculation using the Fukui function[20] for H_2L^3 shows that C3(naphthyl) is softer than C1(naphthyl). Thus, bearing in mind the softness of platinum(II), it seems reasonable that platinum(II) would preferentially bind C3 rather than C1 in H_2L^3. However, the possibility of C1(naphthyl)–H bond activation cannot be ruled out completely in terms of the SHAB principle alone. More exhaustive mechanistic exploration is, therefore, needed to explain these highly regiospecific cycloplatination reactions.

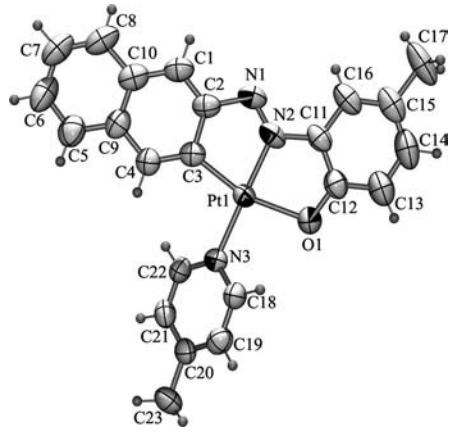

Figure 4. The asymmetric unit of **4a** with displacement ellipsoids drawn at 50% probability. Selected bond lengths [Å] and angles [°]: Pt1–C3 1.980(11), Pt1–N2 1.928(6), Pt1–O1 2.111(8), Pt1–N3 2.035(7), N1–N2 1.265(12), N1–C2 1.422(15), N2–C11 1.440(16), C3–Pt1–N3 101.8(4), N2–Pt1–O1 83.1(4), N2–Pt1–C3 79.4(5), N3–Pt1–O1 95.7(3).

Oxidative Addition Reactions

The addition of halogens to organoplatinum(II) complexes is of historical significance.[21] The fundamental mechanisms of halogen addition to the platinum(II) centre has been elucidated for complexes with nitrogen-donor ligands.[22] Commonly, halogens react with platinum(II) complexes with N-, P-, and As-donor ligands and undergo *trans* oxidative addition.[23] In some cases the platinum(IV) products undergo subsequent isomerization to the thermodynamically stable *cis* isomers.[24]

Compounds **2a** and **2b** undergo smooth oxidation with halogens and methyl iodide in dichloromethane and produce platinum(IV) cyclometallate species **5a**–**6c** in good yields. However, methyl iodide failed to react only with **2b**. In all of these cases oxidative addition took place with concominant $2e^-$ oxidation of Pt^{II} to Pt^{IV} (Scheme 3). Bluish green tetravalent cycloplatinate species of the type $[Pt^{IV}(L)(D)(X_2)]$ containing a Pt^{IV}–C(naphthyl) bond have

been isolated. Products **5a**–**6c** were characterized by elemental analysis and IR and ^{1}H NMR spectroscopy (vide infra). Single crystal X-ray diffraction studies of two representative Pt^{IV} complexes with different Lewis bases **5a** (D = 4-picoline) and **6b** (D = PPh_3) have been undertaken. The ORTEP diagrams with the atom numbering schemes are shown in Figures 5 and 6, respectively. It is noteworthy that *trans* oxidative addition of the halogen has resulted in the case of the cycloplatinate adduct with 4-picoline. The structure of **5a** shows that the platinum(IV) centre is bound to C2 of the naphthyl ring, N2 of the diazene group, O1 of the phenolic fragment of the terdentate donor system and N3 of the 4-picoline donor along with two mutually *trans* iodine atoms occupying the vertices of a distorted octahedron (Figure 5). The Pt(1)–I(1) and Pt(1)–I(2) bond lengths are close to previously reported values.[12a] In contrast, *cis* oxidative addition of the halogen is observed in the corresponding cycloplatinate adduct with PPh_3 **6b** (Figure 6). The coordination geometry around the platinum(IV) centre is distorted octahedral with the two bromine atoms *cis* to each other.

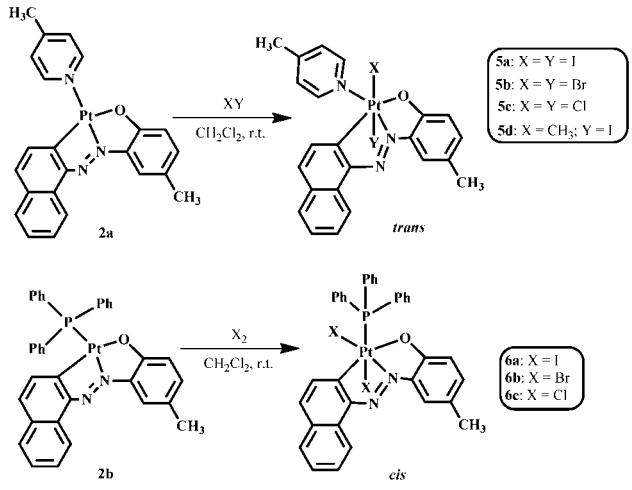

Scheme 3. Oxidative addition reactions of divalent cycloplatinates.

The oxidative addition of alkyl halides and halogens by platinum(II) can proceed by several mechanisms. Depending on the metal substrate, alkyl halide, halogen and reaction conditions, either S_N2 or free radical reactions are possible. A number of studies on oxidative addition of halogens and alkyl halides to square planar platinum(II) complexes have been reported.[25,26] In most cases, reactions of halogens and alkyl halides with square planar d^8 platinum(II) complexes with ligand frames that do not block the vacant axial coordination sites,[27] follow the polar S_N2 pathway and afford kinetically controlled *trans*-platinum(IV) complexes,[26a] although *cis*-products may result after subsequent isomerism.[28] This case provides a unique system where two possible types of oxidative addition reactions have been realized simply by changing the neutral donor ligand (4-picoline and triphenylphosphane). It is reasonable to believe that the 4-picoline–platinum(II) cyclometallate species generates an anion–cation intermediate

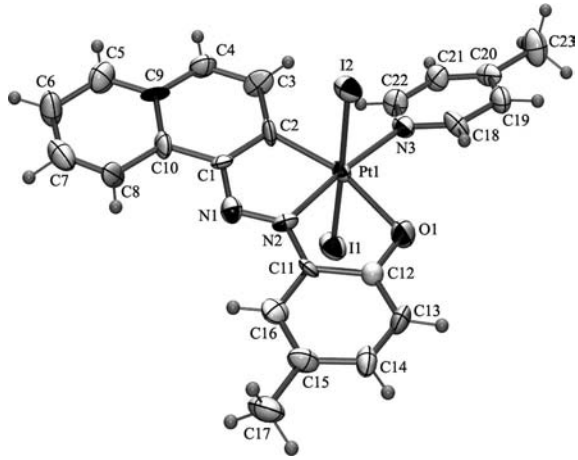

Figure 5. The asymmetric unit of **5a** with displacement ellipsoids drawn at 50% probability. Selected bond lengths [Å] and angles [°]: Pt1–C2 1.979(16), Pt1–N2 1.985(14), Pt1–O1 2.185(12), Pt1–N3 2.061(13), N1–N2 1.267(19), N1–C1 1.380(20), N2–C11 1.330(2), Pt1–I1 2.6407(14), Pt1–I2 2.6522(14), C2–Pt1–N3 105.5(6), N2–Pt1–O1 80.6(5), N2–Pt1–C2 80.0(6), N3–Pt1–O1 93.9(5), C2–Pt1–I1 87.7(5), C2–Pt1–I2 90.6(5).

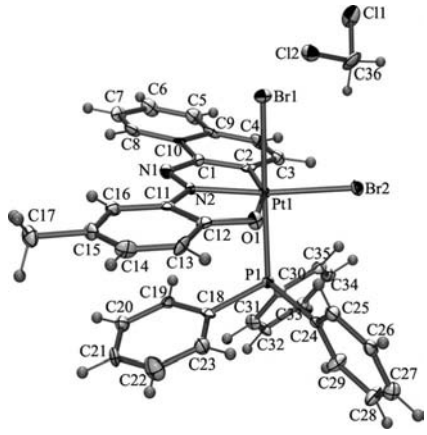

Figure 6. The asymmetric unit of **6b·CH_2Cl_2** with displacement ellipsoids drawn at 50% probability. Selected bond lengths [Å] and angles [°]: Pt1–C2 2.012(7), Pt1–N2 1.965(6), Pt1–O1 2.140(5), Pt1–P1 2.3285(19), N1–N2 1.289(8), N1–C1 1.396(9), N2–C11 1.409(8), Pt1–Br1 2.5042(8), Pt1–Br2 2.4709(8), C2–Pt1–P1 94.62(19), N2–Pt1–O1 81.4(2), N2–Pt1–C2 79.5(3), P1–Pt1–O1 87.22(13), C2–Pt1–Br1 89.25(19), C2–Pt1–Br2 99.3(2).

$[Pt^{II}(L^1)(4\text{-picoline})X]^+X^-$ (X = halogen) in the oxidative reactions by halogens. In the second step, X^- attacks the intermediate *trans* to the metal bound halogen atom. Conversely, it is likely that the corresponding PPh_3–platinum(II) cyclometallate species forms a *trans* addition product initially, followed by rapid rearrangement of the intermediate platinum(IV) complex to the corresponding *cis* isomer, due to the steric bulk of triphenylphosphane. The formation of *cis*-$[Pt^{II}(L^1)(PPh_3)X_2]$ indicates that the *cis* isomer is thermodynamically favoured.

For methyl iodide, the most likely mechanism for the S_N2 reaction is nucleophilic attack on the platinum centre to generate $[Pt^{II}(L^1)(4\text{-picoline})Me]^+I^-$, which rapidly re-

arranges to [Pt^{IV} (L^1)(4-picoline)MeI] (**5d**). The formation of the square pyramidal cationic species in related reactions has already been established,[29] and is thought to be the key intermediate in reactions of methyl iodide and square planar platinum(II) complexes. ESI-MS of **5d** in dichloromethane also gives a similar indication, showing a peak at 563.2274 (100% abundance with correct isotopic pattern) corresponding to the cationic [$Pt^{II}(L^1)$(4-picoline)Me]$^+$ (Supporting Information). Additional information on the structure of **5d** was obtained from NMR spectroscopy (vide infra).

Electronic Spectra and Excited Singlet State Calculations

All the cycloplatinate complexes are soluble in common organic solvents, such as dichloromethane, acetonitrile and acetone, producing either yellowish green (divalent cycloplatinate species) or bluish green solutions (tetravalent cycloplatinate species). Spectral data are presented in Table 1. The electronic spectra of representative divalent cycloplatinate species are shown in Figure 7. The cycloplatinate species show several absorptions in the UV/vis region. The bands appearing in the visible region are generally assigned to metal to ligand [d(Pt)→π (azo)] bands.[12e] Absorptions in the ultraviolet region are attributed to n→π* and π→π* transitions occurring within the ligand orbitals. Various studies by qualitative EHMO calculations have been performed on computer-generated models of related azo complexes.[30] However, to date, no comprehensive theoretical investigations have been made in this regard. This prompted us to use a TD-DFT study to provide an insight into the electronic properties of the platinum(II) compounds. The compounds **2a** and **2b** were chosen as models for the study. Their coordinates were directly imported and single point calculations were performed.

Table 1. Electronic spectroscopic data of **2a**–**6c** in dichloromethane.

	λ_{max} /nm (ε/M^{-1} cm^{-1})
2a	230 (38,500), 260^{sh} (26,200), 310 (21,700), 346 (11,400), 422 (10,400), 776 (4,100), 890 (3,900).
2b	230 (57,000), 310 (19,500), 346 (13,200), 428 (9,800), 800 (4,200), 900 (3,800).
3a	231 (39,700), 395 (12,100), 395 (2,850).
3b	272 (39,500), 400 (8,800), 664 (7,950), 725 (8,200).
4a	230 (35,800), 342 (28,000), 470 (12,700), 500 (14,100), 660 (4,000).
4b	232 (56,500), 346 (32,500), 478 (13,000), 508 (14,500), 676 (5,100).
5a	230 (34,400), 268 (26,200), 392 (8,400), 628 (4,800), 674 (4,600).
5b	231 (36,500), 272 (20,500), 402 (9,200), 630 (8,500), 680 (7,500).
5c	230 (41,600), 630 (7,100), 676 (7,400).
5d	230 (36,100), 626 (5,900), 658 (6,100).
6a	230 (77,300), 296 ^{sh} (38,800), 408 ^{sh} (14,400), 634 (9,000), 682 (10,100).
6b	232 (85,100), 625 (15,600), 680 (12,700).
6c	230 (95,100), 624 (12,500), 676 (13,900).

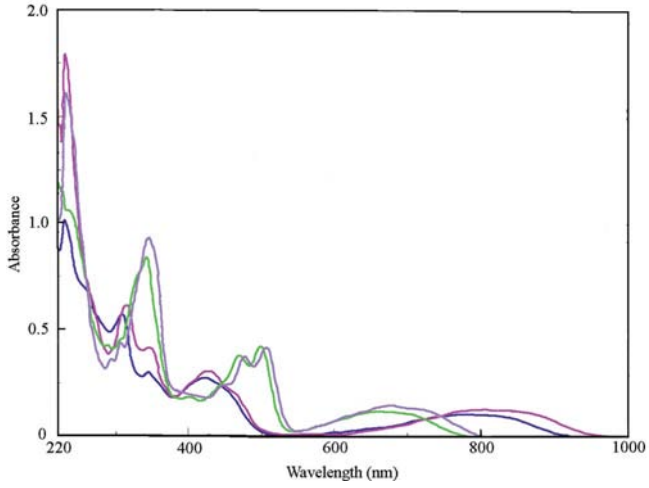

Figure 7. Electronic spectra of **2a** (pink), **2b** (blue), **4a** (green) and **4b** (purple) in dichloromethane.

Orbital Analysis

The divalent cycloplatinate species **2a** and **2b** have similar frontier orbitals (Figure 8 and Supporting Information). The highest occupied molecular orbitals (HOMOs) of **2a** and **2b** are mostly ligand based. The largest orbital contributions in the HOMOs arise from the ligand orbitals, resulting from the combination of the carbon and nitrogen p orbitals with a sizeable percentage of metal d orbitals. HOMO–1 is similar in shape to the HOMO. The HOMO–2 of **2a** has substantial metal d character (36%), and that of **2b** is almost entirely metal based (82% metal character).

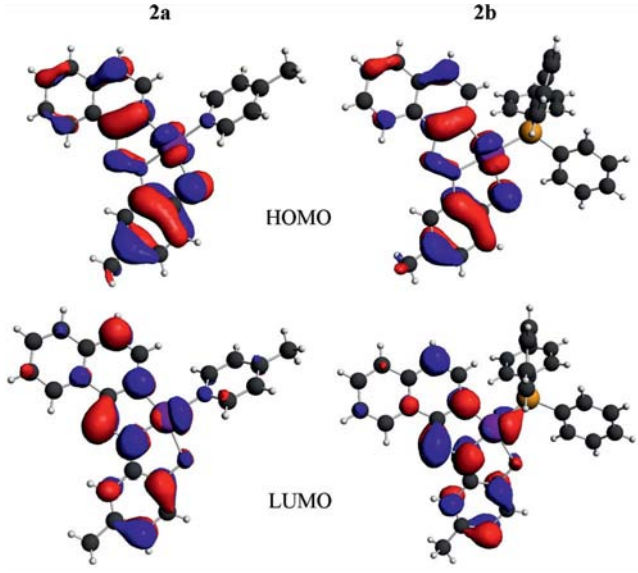

Figure 8. Partial molecular orbital diagram of **2a** and **2b**.

The HOMO–3 of **2a** is very similar to the HOMO–2 of **2b**. The lowest unoccupied molecular orbitals (LUMOs) of the divalent cycloplatinate species are strongly antibonding and localized over the chelating ligand. LUMO+1 in both the platinum(II) complexes is situated over the neutral donors (4-picoline in **2a** and triphenylphosphane in **2b**).

LUMO+2 of **2a** and LUMO+3 of **2b** are also localized over the neutral donors. The HOMO–LUMO gaps in **2a** and **2b** have been computed to be 1.095 and 0.958 eV, repectively. A detailed analysis of the highest occupied and lowest unoccupied molecular orbitals of **2a** and **2b** is compiled in the Supporting Information.

TD-DFT Singlet Transitions

The calculated UV/Vis spectra of **2a** and **2b** are in agreement with those obtained experimentally. The absorption spectra of **2a** obtained using TD-DFT methods showed a number of transitions within the visible and ultraviolet region and good correlation with the experimentally observed spectrum is observed (Tables 2 and 3). The results show that the electronic transition with dominantly contributing configurations involving the HOMO→LUMO orbital pair occurs at 903 nm (first excited state). The experimental spectrum of **2a** in dichloromethane shows a broad peak corresponding to this transition. The broadening of this band could emanate from the mixing of the ligand-to-ligand charge transfer (LLCT) and metal-to-ligand charge transfer (MLCT) transition. The transition involving the HOMO–4→LUMO orbital pair in their dominant configurations appears at 470 nm (sixth excited state) and has been assigned to a mixture of MLCT and LLCT transitions. The other absorptions in the visible region for **2a** have common density redistribution features with a significant amount of MLCT and more or less π–π* intraligand density redistribution. The most intense transition observed for **2a** in the UV region (ca. 260 nm) involves excitation from 75a (HOMO), 74a (HOMO–1), 71a (HOMO–4) and 70a (HOMO–5) to 79a (LUMO+3), 80a (LUMO+4), 84a (LUMO+8) with predominantly intraligand π–π* character. For **2b**, TD-DFT assigns the band centered at 900 nm to LLCT transitions with an admixture of MLCT transitions. The transitions comprising the band at 340 nm are a mixture of intraligand charge transfer (ILCT) and LLCT transitions but TD-DFT underestimates its oscillator strength (*f*).

Table 2. Selected TD-DFT calculations of excitation energies, wavelengths (λ), oscillator strengths (*f*) and compositions of the low-lying singlet states for **2a** in dichloromethane.

State	Energy [eV]	λ_{cal} [nm]	λ_{exp} [nm]	*f*	Composition	Character
S_1	1.3735	903	890	0.047	HOMO→LUMO (97.2%)	ILCT+MLCT
S_6	2.6382	470	422	0.115	HOMO–4→LUMO (79.7%)	MLCT+LLCT
S_{10}	3.2894	377	–	0.137	HOMO–6→LUMO (84%)	ILCT+MLCT
S_{13}	3.5623	348	–	0.215	HOMO→LUMO+4 (63.4%) HOMO–8→LUMO (11.3%)	ILCT+MLCT
S_{19}	3.7263	333	310	0.073	HOMO–4→LUMO+1 (40.4%) HOMO–2→LUMO+1 (25.9%) HOMO–8→LUMO (18.1%)	MLCT+ILCT
S_{32}	4.344	285	–	0.059	HOMO–6→LUMO+1 (31.8%) HOMO–11→LUMO (19.7%) HOMO–1→LUMO+4 (17.7%) HOMO–5→LUMO+1 (12.9%)	ILCT+LLCT+MLCT
S_{45}	4.7549	260	260	0.158	HOMO–1→LUMO+4 (18.7%) HOMO→LUMO+8 (15.3%) HOMO–4→LUMO+4 (9.3%) HOMO–5→LUMO+4 (8.5%) HOMO–4→LUMO+3 (8.4%)	LLCT+ILCT+ MLCT
S_{69}	5.3104	233	230	0.067	HOMO–11→LUMO+1 (36%) HOMO–3→LUMO+5 (23.2%) HOMO–5→LUMO+4 (9.3%)	LLCT+MLCT

Table 3. Selected TD-DFT calculations of excitation energies, wavelengths (λ), oscillator strengths (*f*) and compositions of the low-lying singlet states for **2b** in dichloromethane.

State	Energy [eV]	λ_{cal} [nm]	λ_{exp} [nm]	*f*	Composition	Character
S_1	1.2060	1028	900	0.136	HOMO→LUMO (97.4%)	ILCT+MLCT
S_5	2.4974	495	–	0.069	HOMO–4→LUMO (64.1%) HOMO–5→LUMO (19.2%)	MLCT+LLCT
S_{19}	3.3103	375	428	0.072	HOMO→LUMO+6 (65.7%) HOMO–13→LUMO (14.2%)	ILCT+MLCT
S_{24}	3.6446	340	346	0.020	HOMO→LUMO+2 (93.3%)	ILCT+LLCT
S_{59}	4.5332	270	–	0.012	HOMO–5→LUMO+2 (42.0%) HOMO–5→LUMO+3 (18.3%) HOMO–7→LUMO+2 (11.8%)	LLCT +ILCT MLCT

Conclusions

This study shows that naphthylazo-2′-hydroxyarene ligands (**1**) undergo regiospecific cyclometallation reactions mediated by the allyl platinum(II) complex $[(\eta^3\text{-}C_4H_7)Pt(\mu\text{-}Cl)]_2$. The position of the primary donor (diazene group) was found to dictate the sites of metallation. Exclusive C2(naphthyl)–H bond activation has been achieved when the diazene group is at C1 and the auxiliary donor is phenol or naphthol. On the other hand, exclusive C3(naphthyl)–H bond activation has been observed in H_2L^3, where the primary donor is attached to the C2 atom. The regiospecificity in these cases can be explained in terms of five-membered carboplatinacycle ring formation followed by N,O-chelation. The square planar bivalent cycloplatinate species are shown to undergo oxidative addition reactions with halogens and methyl iodide affording air-stable platinum(IV) compounds. The influence of the steric bulk of the donor molecules (D) on the stereochemistry of the oxidized products has been observed. Here both *cis* and *trans* addition of the electrophiles have been achieved using different D. The electronic and UV/Vis spectroscopic properties of the representative platinum(II) complexes in dichloromethane have been investigated by TD-DFT calculations.

Experimental Section

General Remarks: C, H and N elemental analyses were performed with either Perkin–Elmer (Model 240C) or Heraeus Carlo–Erba 1108 elemental analyzers. IR spectra were obtained with a Jasco 5300 FT-IR. Visible and ultraviolet spectra were recorded with a Jasco V-530 spectrophotometer. ^{1}H NMR spectra were measured in $CDCl_3$ with a Bruker Avance DPX 300 NMR spectrometer with $SiMe_4$ as an internal standard. The FAB mass spectra were recorded with a JEOL SX 102/DA-6000 Mass Spectrometer/Data System using Argon/Xenon (6 kV, 10 mA) as the FAB gas. ESI mass spectra were recorded with a Micromass Quattro II triple quadrupole mass spectrometer. $K_2[PtCl_4]$ was obtained from Arora-Matthey, Kolkata. $[(\eta^3\text{-}C_4H_7)Pt(\mu\text{-}Cl)]_2$ was prepared following a reported method.[31] Solvents and chemicals were of analytical grade. H_2L^1–H_2L^3 were prepared according to a published procedure.[32]

1-(2′-Hydroxy-5′-methylphenylazo)naphthalene (H_2L^1): Yield 65%. $C_{17}H_{15}N_2O$ (263.12): calcd. C 77.84, H 5.38, N 10.68; found C 79.95, H 4.52, N 9.31. ^{1}H NMR (300 MHz, $CDCl_3$): δ = 6.90 (d, 1 H, J = 9.4 Hz), 7.40 (t, 1 H), 7.55–7.66 (m, 5 H), 7.73–7.82 (m, 2 H), 7.90 (d, 1 H, J = 8.1 Hz), 8.19 (d, 1 H, J = 7.5 Hz), 8.32 (d, 1 H, J = 8.3 Hz), 8.62 (d, 1 H, J = 8.1 Hz), 17.23 (s, 1 H, OH) ppm.

1-(2′-Hydroxynaphthylazo)naphthalene (H_2L^2): Yield 75%. $C_{20}H_{14}N_2O$ (298.34): calcd. C 80.52, H 4.73, N 9.39; found C 80.25, H 4.52, N 9.47. ^{1}H NMR (300 MHz, $CDCl_3$): δ = 6.89 (d, 1 H, J = 9.3 Hz), 7.37–7.62 (m, 5 H), 7.70 (d, 1 H, J = 9.3 Hz), 7.83–8.06 (m, 5 H), 8.62 (d, 1 H, J = 8.0 Hz), 16.34 (s, 1 H, OH) ppm.

2-(2′-Hydroxy-5′-methylphenylazo)naphthalene (H_2L^3): Yield 55%. $C_{17}H_{15}N_2O$ (263.12): calcd. C 77.84, H 5.38, N 10.68; found C 78.02, H 5.51, N 10.41. ^{1}H NMR (300 MHz, $CDCl_3$): δ = 1.54 (s, 3 H, 5′-Me) 6.90 (d, 1 H, J = 8.6 Hz), 7.26 (d, 1 H, J = 8.1 Hz), 7.40–7.65 (m, 6 H), 8.25 (d, 1 H, J = 8.1 Hz), 8.81 (d, 1 H, J = 8.6 Hz), 16.30 (s, 1 H, OH) ppm.

[Pt(L^1)(4-picoline)] (2a): H_2L^1 (0.025 g, 0.0954 mmol) was added to a solution of $[(\eta^3\text{-}C_4H_7)Pt(\mu\text{-}Cl)]_2$ (0.027 g, 0.0477 mmol) in chloroform (15 mL). Compound **2a** was isolated following the two work up procedures outlined below.

(i) The reaction mixture was stirred magnetically for 8 h and a solution of 4-picoline (0.088 g, 0.954 mmol) in chloroform (5 mL) was added to the solution. The greenish solution was stirred for a further 2 h. The solution was then filtered, washed with chloroform (4 × 5 mL) and the solvent evaporated. The crude product was dissolved in CH_2Cl_2 and preparative TLC was performed on a silica gel plate with petroleum ether (60–80 °C)/ethyl acetate (4:1, v/v) as eluent. The green band was isolated and extracted with acetone. Removal of acetone gave **2a**; yield 75%. $C_{23}H_{19}N_2OPt$ (534.23): calcd. C 50.36, H 3.49, N 7.66; found C 50.49, H 3.32, N 7.58%. ^{1}H NMR ($CDCl_3$):δ: 2.34 (s, 3 H, aryl CH_3), 2.42 (s, 3 H, CH_3 of 4-picoline); aromatic protons: 6.95–8.00. IR (KBr): $\tilde{\nu}$ = 1410 (–N=N–) cm^{-1}. MS: *m*/*z* 548 [M]$^+$.

(ii) The reaction mixture was layered on a preparative silica gel plate. The plate was then heated in an air-oven at 120 °C for 6 hours. The desired product was the isolated by eluting the silica plates with 10% 4-picoline in petroleum ether (60–80 °C)/ethyl acetate (4:1, v/v); yield 70%.

[Pt(L^1)(PPh_3)] (2b): Complex **2b** was synthesized a method similar to that used for **2a** using triphenylphosphane instead of 4-picoline; yield 70%. $C_{35}H_{27}N_2OPPt$ (717.67): calcd. C 58.58, H 3.79, N 3.90; found C 58.71, H 3.82, N 4.01. ^{1}H NMR ($CDCl_3$): δ = 2.18 (s, 3 H, aryl CH_3), aromatic protons: 6.10–6.14 (dd, J = 8.4 Hz, 1 H), 6.35 (d, J = 8.7 Hz, 1 H), 6.76–6.80 (dd, J = 8.7 Hz, 1 H), 6.87 (d, J = 8.4 Hz, 1 H), 7.03 (s, 1 H), 7.23–7.32 (m, 5 H), 7.38–7.50 (m, 8 H), 7.60–7.73 (m, 5 H), 8.40 (d, J = 8.1 Hz, 1 H) ppm. IR (KBr): $\tilde{\nu}$ = 1405 (–N=N–) cm^{-1}. MS: *m*/*z* 718 [M]$^+$.

The cycloplatinates **3a**, **3b**, **4a** and **4b** were synthesized following the method used for **2a** and **2b**.

[Pt(L^2)(4-picoline)] (3a): Yield 65%. $C_{26}H_{19}N_3OPt$ (584.55$_3$): δ = 2.52 (s, 3 H, CH_3 of 4-picoline); aromatic protons: 6.80 (d, J = 8.7 Hz, 1 H), 7.12 (d, J = 9.3 Hz, 1 H), 7.25 (d, J = 10.2 Hz, 2 H), 7.30–7.45 (m, 5 H), 7.48–7.60 (m, 4 H), 7.81 (m, 2 H), 8.6 (d, J = 8.6 Hz, 1 H) ppm. IR (KBr): $\tilde{\nu}$ = 1410 (–N=N–) cm^{-1}. MS: *m*/*z* 585 [M]$^+$.

[Pt(L^2)(PPh_3)] (3b): Yield 62%. $C_{38}H_{27}N_2OPPt$ (753.71): calcd. C 60.56, H 3.61, N 3.72; found C 60.42, H 3.65, N 3.84. ^{1}H NMR ($CDCl_3$): δ = aromatic protons: 6.78 (d, J = 8.7 Hz, 1 H), 7.05 (d, J = 9.0 Hz, 1 H), 7.22–7.56 (m, 15 H), 7.71–7.85 (m, 6 H), 7.92 (m, 2 H), 8.06 (m, 2 H), 8.6 (d, J = 9.0 Hz, 1 H) ppm. IR (KBr): $\tilde{\nu}$ = 1412 (–N=N–) cm^{-1}. MS: *m*/*z* 753 [M]$^+$.

[Pt(L^3)(4-picoline)] (4a): Yield 68%. $C_{23}H_{19}N_2OPt$ (534.51): calcd. C 50.36, H 3.49, N 7.66; found C 50.41, H 3.56, N 7.64. ^{1}H NMR ($CDCl_3$): δ = 2.14 (s, 3 H, aryl CH_3), 2.50 (s, 3 H, CH_3 of 4-picoline); aromatic protons: 6.62–6.69 (t, 2 H), 6.98 (d, J = 8.7 Hz, 1 H), 7.26–7.42 (m, 6 H), 7.62 (d, J = 8.3 Hz, 1 H), 7.82 (s, 1 H), 8.77 (d, 2 H) ppm. IR (KBr): $\tilde{\nu}$ = 1405 (–N=N–) cm^{-1}. MS: *m*/*z* 548 [M]$^+$.

[Pt(L^3)(PPh_3)] (4b): Yield 65%. $C_{38}H_{27}N_2OPPt$ (753.71): calcd. C 60.56, H 3.61, N 3.72; found C 60.55, H 3.51, N 3.81. ^{1}H NMR ($CDCl_3$): δ = 2.17 (s, 3 H, aryl CH_3); aromatic protons: 6.54 (d, J = 8.7 Hz, 1 H), 6.71 (d, J = 8.7 Hz, 1 H), 6.93 (d, J = 8.7 Hz, 1 H), 7.07–7.20 (m, 3 H), 7.39–7.54 (m, 10 H), 7.65–7.72 (m, 8 H) ppm. IR (KBr): $\tilde{\nu}$ = 1415 (–N=N–) cm^{-1}. MS: *m*/*z* 718 [M]$^+$.

General Procedure for the Oxidative Addition of Electrophiles to Divalent Cycloplatinates: A dichloromethane solution of the halogen or methyl iodide (1%) was added dropwise to a dichloromethane solution (10 mL) of the Pt^{II} complex (0.055 mmol) with stirring until the yellowish green colour of the reaction mixture changed to bluish green. The mixture was stirred for a further 1 h to ensure the complete disappearance of the starting materials. The solvent was evaporated and the crude product was dissolved in a minimum quantity of dichloromethane and subjected to purification by TLC on silica gel with petroleum ether (60–80 °C)/ethyl acetate (10:1, v/v) as eluent to afford **5a**–**6c**.

[Pt(L¹)(4-picoline)I₂] (5a): Yield 66%. $C_{23}H_{19}I_2N_3OPt$ (802.32): calcd. C 34.43, H 2.39, N 5.24; found C 34.28, H 2.40, N 5.56. ^1H NMR ($CDCl_3$): δ = 2.34 (s, 3 H, aryl CH_3), 2.55 (s, 3 H, CH_3 of 4-picoline); aromatic protons: 6.84 (d, J = 9 Hz, 1 H), 7.08 (d, J = 9.3 Hz, 1 H), 7.17 (d, J = 10.2 Hz, 1 H), 7.20–7.77 (m, 5 H), 7.80 (d, J = 7.8 Hz, 1 H), 7.88 (d, J = 8.1 Hz, 1 H), 8.62 (d, J = 7.8 Hz, 1 H), 9.36 (m, 2 H) ppm. IR (KBr): $\tilde{\nu}$ = 1400 (–N=N–) cm^{-1}. MS: m/z 802 $[M]^+$, 548 $[M - 2I]^+$.

[Pt(L¹)(4-picoline)Br₂] (5b): Yield 70%. $C_{23}H_{19}Br_2N_3OPt$ (708.32): calcd. C 39.00, H 2.70, N 5.93; found C 38.95, H 2.81, N 5.84. ^1H NMR ($CDCl_3$): δ = 2.31 (s, 3 H, aryl CH_3), 2.58 (s, 3 H, CH_3 of 4-picoline); aromatic protons: 7.10 (d, J = 8.7 Hz, 1 H), 7.36–7.49 (m, 6 H), 7.55–7.59 (m, 1 H), 7.74 (d, J = 8.6 Hz, 1 H), 7.85 (d, J = 8.2 Hz, 1 H), 8.62 (d, J = 8.3 Hz, 1 H), 9.17 (m, 2 H) ppm. IR (KBr): $\tilde{\nu}$ = 1402 (–N=N–) cm^{-1}. MS: m/z 706 $[M]^+$, 548 $[M - 2Br]^+$.

[Pt(L¹)(4-picoline)Cl₂] (5c): Yield 62%. $C_{23}H_{19}Cl_2N_3OPt$ (619.42): calcd. C 44.60, H 3.09, N 6.78; found C 44.51, H 3.21, N 7.01. ^1H NMR ($CDCl_3$): δ = 2.26 (s, 3 H, aryl CH_3), 2.66 (s, 3 H, CH_3 of 4-picoline); aromatic protons: 6.4–9.3 (br) ppm. IR (KBr): $\tilde{\nu}$ = 1405 (–N=N–) cm^{-1}. MS: m/z 619 $[M]^+$, 548 $[M - 2Cl]^+$.

[Pt(L¹)(4-picoline)(CH₃)(I)] (5d): Yield 72%. $C_{24}H_{22}IN_3OPt$ (690.45): calcd. C 41.7, H 3.2, N 6.1; found C 41.8, H 3.3, N 6.1. ^1H NMR ($CDCl_3$): δ = 1.8 (t, $J_{Pt\text{-}H}$ = 63 Hz, 3 H, Pt-CH_3), 2.33 (s, 3 H, aryl CH_3), 2.55 (s, 3 H, CH_3 of 4-picoline); aromatic protons: 6.8 (d, J = 9.0 Hz, 1 H), 7.0 (d, J = 9.0 Hz, 1 H), 7.2 (d, J = 9.0 Hz, 1 H), 7.4–7.7 (m, 5 H), 7.8 (d, J = 8.1 Hz, 1 H), 8.6 (d, J = 8.4 Hz, 2 H), 9.1 (m, 2 H) ppm. IR (KBr): $\tilde{\nu}$ = 1410 (–N=N–) cm^{-1}. MS: m/z 690 $[M]^+$, 564 $[M - I]^+$. ESI-MS: 563.2274 [M – I] (calculated mass: 563.1411).

[Pt(L¹)(PPh₃)I₂] (6a): Yield 70%. $C_{35}H_{27}I_2N_2OPPt$ (971.48): calcd. C 43.27, H 2.80, N 2.88; found C 43.16, H 2.59, N 2.90. ^1H NMR ($CDCl_3$): δ = 2.12 (s,3 H, aryl CH_3); aromatic protons: 6.34–8.48 ppm. IR (KBr): $\tilde{\nu}$ = 1410 (–N=N–) cm^{-1}. MS: m/z 971 $[M]^+$, 718 $[M - 2I]^+$.

[Pt(L¹)(PPh₃)Br₂] (6b): Yield 75%. $C_{35}H_{27}Br_2N_2OPPt$ (877.48): calcd. C 47.91, H 3.10, N 3.19; found C 48.05, H 2.98, N 3.15. ^1H NMR ($CDCl_3$): δ = 2.18 (s, 3 H, aryl CH_3); aromatic protons: 6.42 (d, J = 9.0 Hz, 1 H), 6.53 (d, J = 8.7 Hz, 1 H), 6.84 (m, 2 H), 7.10 (s, 1 H), 7.17–7.48 (m, 15 H), 7.58 (dd, 1 H), 8.39 (d, J = 7.8 Hz, 1 H), 8.69 (d, J = 8.7 Hz, 1 H) ppm. IR (KBr): $\tilde{\nu}$ = 1406 (–N=N–) cm^{-1}. MS: m/z 878 $[M]^+$, 718 $[M - 2Br]^+$.

[Pt(L¹)(PPh₃)Cl₂] (6c): Yield 68%. $C_{35}H_{27}Cl_2N_2OPPt$ (788.58): calcd. C 53.31, H 3.45, N 3.55; found C 53.42, H 3.41, N 3.70. ^1H NMR ($CDCl_3$): δ = 2.17 (s,3 H, aryl CH_3); aromatic protons: 6.65–8.61 (br) ppm. IR (KBr): $\tilde{\nu}$ = 1412 (–N=N–) cm^{-1}. MS: m/z 788 $[M]^+$, 718 $[M - 2Cl]^+$.

Table 4. Crystallographic data and experimental details for **2a**, **2b**, **3a**, **4a**, **5a** and **6b**.

	2a	**2b**	**3a**	**4a**	**5b**	**6b**
Empirical formula	$C_{23}H_{19}N_3OPt$	$C_{35}H_{27}N_2OPPt$	$C_{26}H_{19}N_3OPt$	$C_{23}H_{19}N_3OPt$	$C_{23}H_{19}I_2N_3OPt$	$C_{36}H_{29}N_2$ Br_2OPPt
Formula weight	548.50	717.67	584.54	548.50	802.30	962.39
Temperature	293(2) K	293(2) K	293(2) K	293(2) K	293(2) K	293(2) K
Crystal system	monoclinic	triclinic	monoclinic	monoclinic	monoclinic	monoclinic
Space group	$P2_1/c$	$P\bar{1}$	$P2_1/c$	$P2_1$	$P2_1/c$	$C2/c$
Unit cell dimensions	a = 15.723(19) Å b = 7.9134(9) Å c = 17.345(2) Å α = 90° β = 112.081(2)° γ = 90°	a = 9.7817(11) Å b = 10.6325(12) Å c = 14.3017(16) Å α = 78.877(2)° β = 83.8270(10)° γ = 68.5090(10)°	a = 15.173(5) Å b = 7.445(2) Å c = 18.396(6) Å α = 90° β = 101.528(5)° γ = 90°	a = 10.1763(9) Å b = 7.4642(6) Å c = 13.2483(11) Å α = 90° β = 102.3970(10)° γ = 90°	a = 13.488(3) Å b = 14.095(3) Å c = 14.236(3) Å α = 90° β = 111.218(4)° γ = 90	a = 33.230(3) Å b = 1.5207(10) Å c = 22.438(2) Å α = 90° β = 128.435(2)° γ = 90°
Volume	1999.9(4) A^3	1356.9(3) A^3	2036.0(11) A^3	982.85(14) A^3	2522.9(10) A^3	6728.8(11) A^3
Z, d_{calc} [Mg/m^3]	4, 1.822	2, 1.757	4, 1.907	2, 1.853	4, 2.112	8, 1.900
Abs. coefficient	7.034 mm^{-1}	5.262 mm^{-1}	6.916 mm^{-1}	7.156 mm^{-1}	8.027 mm^{-1}	6.785 mm^{-1}
F(000)	1056	704	1128	528	1480	3712
Crystal size	0.42×0.22×0.11	0.45×0.36×0.23	0.25×0.18×0.10	0.44×0.18×0.04	0.36×0.25×0.19	0.32×0.24×0.18
Theta range for data collection	1.40 to 25.00°	2.24 to 25.00°	1.37 to 25.00°	1.57 to 24.98°	2.11 to 25.00°	1.93 to 26.00°
Limiting indices	$-18 \le h \le 18$ $-9 \le k \le 9$ $-20 \le l \le 20$	$-11 \le h \le 11$ $-11 \le k \le 12$ $-16 \le l \le 16$	$-18 \le h \le 18$ $-8 \le k \le 8$ $-21 \le l \le 21$	$-12 \le h \le 12$ $-8 \le k \le 8$ $-15 \le l \le 15$	$-16 \le h \le 16$ $-16 \le k \le 16$ $-16 \le l \le 16$	$-20 \le h \le 40$ $-14 \le k \le 14$ $-27 \le l \le 19$
Reflections collected/unique	18179/3520 [R(int) = 0.0277]	7551/4714 [R(int) = 0.0288]	18304/3567 [R(int) = 0.0452]	9416/3436 [R(int) = 0.0267]	22325/4338 [R(int) = 0.0695]	18761/6609 [R(int) = 0.0607]
Data/restraints/parameters	3520/0/255	4714/0/362	3567/0/281	3436/1/255	4338/0/268	6609/0/402
Goof on F^2	1.114	1.022	1.069	1.077	1.190	1.042
Final R indices [$I>2\sigma(I)$]	$R1$ = 0.0411 $wR2$ = 0.1218	$R1$ = 0.0295 $wR2$ = 0.0661	$R1$ = 0.0314 $wR2$ = 0.0655	$R1$ = 0.0356 $wR2$ = 0.0958	$R1$ = 0.0846 $wR2$ = 0.1732	$R1$ = 0.0470 $wR2$ = 0.0921
R indices (all data)	$R1$ = 0.0460 $wR2$ = 0.1295	$R1$ = 0.0326 $wR2$ = 0.0673	$R1$ = 0.0396 $wR2$ = 0.0686	$R1$ = 0.0376 $wR2$ = 0.0974	$R1$ = 0.1042 $wR2$ = 0.1816	$R1$ = 0.0647 $wR2$ = 0.0972
Largest diff. peak and hole ($e \cdot A^{-3}$)	4.130 and –1.044	1.582 and –0.742	0.786 and –0.519	0.891 and –0.475	4.217 and –2.860	1.544 and –1.731

X-ray Crystallography: Crystallographic data and experimental details for **2a**, **2b**, **3a**, **4a**, **5a** and **6b** are summarized in Table 4. Data were collected with a Bruker SMART 1000 CCD area-detector diffractometer using graphite monochromated Mo-K_α (λ = 0.71073 Å) radiation by ω scan. The structures were solved by direct methods using SHELXS-97[33] and difference Fourier syntheses and refined with SHELXL-97 incorporated in WinGX 1.64 crystallographic collective package.[34] All the hydrogen positions for the compound were initially located in the difference Fourier map, and for the final refinement, the hydrogen atoms were placed geometrically and held in the riding mode. The last cycles of refinement included atomic positions for all the atoms, anisotropic thermal parameters for all non-hydrogen atoms and isotropic thermal parameters for all the hydrogen atoms. Full-matrix-least-squares structure refinement against $|F^2|$. Molecular geometry calculations were performed with PLATON,[35] and molecular graphics were prepared using ORTEP-3.[36]

CCDC-823076 (for **2a**), -823077 (for **2b**), -823078 (for **3a**), -823079 (for **4a**), -823080 (for **5a**) and -823081 (for **6b**) contain the supplementary crystallographic data for this paper. These data can be obtained free of charge from The Cambridge Crystallographic Data Centre via www.ccdc.cam.ac.uk/data_request/cif.

Computational Details: Calculations were performed with the TD-DFT formalism as implemented in ADF2007.[37] Two approximations were generally made for the XC potential and for the XC kernel, which is the functional derivative of the TD XC potential with respect to density. We used the local density approximation including the VWN parametrization[38] in the SCF step and Becke[39] and Perdew–Wang[40] gradient corrections to the exchange and correlation, respectively, and adiabatic local density approximation (ALDA) for the XC kernel, in the post-SCF step. TD-DFT calculations have been performed with the uncontracted triple-STO basis set with a polarization function for all atoms. In the calculation of the optical spectra, 70 lowest spin-allowed singlet-singlet transitions were taken into account. Transition energies and oscillator strengths were interpolated by a Gaussian convolution with a σ of 0.2 eV. Solvent effects were modelled by the conductor-like screening model[41] of solvation as implemented in ADF.

Regioselectivity for subsequent metallation at different C(naphthyl)–H bonds was ascertained through evaluation of the Fukui function.[24] For the calculation of condensed Fukui function values, gradient corrected BLYP with LDA VWN correlation potential methods were used for the computations. All the structures have been optimized with the gradient corrected BLYP method, with LDA VWN[38] correlation functionals. The Huzinaga double-zeta basis set[42] with polarization was used. Single point energy calculations were performed at the above level of theory for the cations of the conformers using the ground state optimized structures. The individual atomic charges (gross charge) calculated by Mulliken population analysis were used to calculated the condensed Fukui functions using ADF.

Supporting Information (see footnote on the first page of this article): ESI-MS spectrum of **5d**, description of crystal packing of the cycloplatinate species and details of TD-DFT calculations

Acknowledgments

Financial assistance received from the Department of Science and Technology (DST), Government of India, New Delhi is gratefully acknowledged.

[1] a) M. Albrecht, *Chem. Rev.* **2010**, *110*, 576–623; b) G. Dyker, *Angew. Chem.* **1999**, *111*, 1808; *Angew. Chem. Int. Ed.* **1999**, *38*, 1698–1712; c) Y. Guari, S. Sabo-Etienne, B. Chaudret, *Eur. J. Inorg. Chem.* **1999**, 1047–1055; d) V. Ritleng, C. Sirlin, M. Pfeffer, *Chem. Rev.* **2002**, *102*, 1731–1770; e) A. D. Ryabov, *Chem. Rev.* **1990**, *90*, 403–424; f) B. A. Arndtsen, R. G. Bergman, T. A. Mobley, T. H. Peterson, *Acc. Chem. Res.* **1995**, *28*, 154–162.

[2] a) J. Dupont, C. S. Consorti, J. Spencer, *Chem. Rev.* **2005**, *105*, 2527–2571; b) M. E. van der Boom, D. Milstein, *Chem. Rev.* **2003**, *103*, 1759–1792; c) M. Albrecht, G. van Koten, *Angew. Chem.* **2001**, *113*, 3866; *Angew. Chem. Int. Ed.* **2001**, *40*, 3750–3781.

[3] a) R. H. Crabtree, *J. Chem. Soc., Dalton Trans.* **2001**, 2437–2450; b) C. Jia, T. Kitamura, Y. Fujiwara, *Acc. Chem. Res.* **2001**, *34*, 633–639.

[4] a) W. Baratta, S. Stoccoro, A. Doppiu, E. Herdtweck, A. Zucca, P. Rigo, *Angew. Chem.* **2003**, *115*, 109; *Angew. Chem. Int. Ed.* **2003**, *42*, 105–109; b) A. G. Wong-Foy, L. M. Henling, M. Day, J. A. Labinger, J. E. Bercaw, *J. Mol. Catal. A* **2002**, *189*, 3–16.

[5] a) H. A. Zhong, J. A. Labinger, J. E. Bercaw, *J. Am. Chem. Soc.* **2002**, *124*, 1378–1399; b) A. Zucca, A. Doppiu, M. A. Cinellu, S. Stoccoro, G. Minghetti, M. Manassero, *Organometallics* **2002**, *21*, 783–785; c) J. C. Thomas, J. C. Peters, *J. Am. Chem. Soc.* **2001**, *123*, 5100–5101.

[6] a) J. Kua, X. Xu, R. A. Periana, W. A. Goddard III, *Organometallics* **2002**, *21*, 511–525; b) J. Procelewska, A. Zahl, R. van Eldik, H. A. Zhong, J. A. Labinger, J. E. Bercaw, *Inorg. Chem.* **2002**, *41*, 2808–2810.

[7] a) S. Develay, J. A. G. Williams, *Dalton Trans.* **2008**, 4562–4564; b) K. E. Dungey, B. D. Thompson, N. A. P. Kane-Maguire, L. L. Wright, *Inorg. Chem.* **2000**, *39*, 5192–5196; c) J. A. G. Williams, A. Beeby, E. S. Davies, J. A. Weinstein, C. Wilson, *Inorg. Chem.* **2003**, *42*, 8609–8611; d) V. W.-W. Yam, R. P.-L. Tang, K. M.-C. Wong, X.-X. Lu, K.-K. Cheung, N. Zhu, *Chem. Eur. J.* **2002**, *8*, 4066–4076.

[8] a) W. V. Konze, B. L. Scott, G. J. Kubas, *J. Am. Chem. Soc.* **2002**, *124*, 12550–12556; b) M. Albrecht, A. L. Spek, G. van Koten, *J. Am. Chem. Soc.* **2001**, *123*, 7233–7246.

[9] a) M. Ghedini, D. Pucci, A. Crispini, G. Barberio, *Organometallics* **1999**, *18*, 2116–2124; b) E. Steiner, F. A. L'Eplattenier, *Helv. Chim. Acta* **1978**, *61*, 2264–2268.

[10] a) C. F. O'Neill, B. Koberle, J. R. W. Masters, L. R. Kelland, *Br. J. Cancer* **1999**, *81*, 1294–1303; b) P. Köff-Maier, H. Köff, *Chem. Rev.* **1987**, *87*, 1137–1152.

[11] A. C. Cope, R. W. Siekman, *J. Am. Chem. Soc.* **1965**, *87*, 3272–3273.

[12] a) J. W. Slater, J. P. Rourke, *J. Organomet. Chem.* **2003**, *688*, 112–120; b) A. Caubet, C. López, X. Solans, M. Font-Bardia, *J. Organomet. Chem.* **2003**, *669*, 164–171; c) C. Larraz, R. Navarro, E. P. Urriolabeitia, *New J. Chem.* **2000**, *24*, 623–630; d) R. A. Gossage, A. D. Ryabov, A. L. Spek, D. J. Stufkens, J. A. M. van Beek, R. van Eldik, G. van Koten, *J. Am. Chem. Soc.* **1999**, *121*, 2488–2497; e) S. Chattopadhyay, C. Sinha, P. Basu, A. Chakravorty, *Organometallics* **1991**, *10*, 1135–1139; f) T. Kawamoto, I. Nagasawa, H. Kuma, Y. Kushi, *Inorg. Chim. Acta* **1997**, *265*, 163–167; g) C. M. Anderson, M. Crespo, G. Ferguson, A. J. G. Lough, R. J. Puddephatt, *Organometallics* **1992**, *11*, 1177–1181.

[13] a) T. Kawamoto, I. Nagasawa, H. Kuma, Y. Kushi, *Inorg. Chem.* **1996**, *35*, 2427–2432; b) E. Wehman, G. van Koten, C. T. Knaap, H. Ossor, M. Pfeffer, A. L. Spek, *Inorg. Chem.* **1988**, *27*, 4409–4417; c) J. M. Duff, B. E. Mann, B. L. Shaw, B. Turtle, *J. Chem. Soc., Dalton Trans.* **1974**, 139–145.

[14] a) M. P. Brown, R. J. Puddephatt, C. E. E. Upton, *J. Chem. Soc., Dalton Trans.* **1974**, 2457–2465; b) S. Roy, R. J. Puddephatt, J. D. Scott, *J. Chem. Soc., Dalton Trans.* **1989**, 2121–

2125; c) M. P. Brown, R. J. Puddephatt, C. E. E. Upton, *J. Chem. Soc., Dalton Trans.* **1973**, *49*, C61–5.
[15] a) K. I. Goldberg, J. Yan, E. L. Winter, *J. Am. Chem. Soc.* **1994**, *116*, 1573–1574; b) K. I. Goldberg, J. Yan, E. M. Breitung, *J. Am. Chem. Soc.* **1995**, *117*, 6889–6896; c) B. S. Williams, A. W. Holland, K. I. Goldberg, *J. Am. Chem. Soc.* **1999**, *121*, 252–253; d) B. S. Williams, K. I. Goldberg, *J. Am. Chem. Soc.* **2001**, *123*, 2576–2587; e) D. M. Crumpton, K. I. Goldberg, *J. Am. Chem. Soc.* **2000**, *122*, 962–963; f) D. M. Crumpton-Bregel, K. I. Goldberg, *J. Am. Chem. Soc.* **2003**, *125*, 9442–9456; g) P. Procelewska, A. Zahl, G. Liehr, R. van Eldik, N. A. Smythe, B. S. Williams, K. I. Goldberg, *Inorg. Chem.* **2005**, *44*, 7732–7742.
[16] a) G. van Koten, K. Timmer, J. G. Noltes, A. L. Spek, *J. Chem. Soc., Chem. Commun.* **1978**, 250–252; b) D. M. Grove, G. van Koten, H. J. C. Ubbels, A. L. Spek, *J. Am. Chem. Soc.* **1982**, *104*, 4285–4286; c) A. F. M. van der Ploeg, G. van Koten, K. Vrieze, *J. Organomet. Chem.* **1981**, *222*, 155–174; d) D. M. Grove, G. van Koten, H. J. C. Ubbels, *Organometallics* **1982**, *1*, 1366–1370; e) D. M. Grove, G. van Koten, J. N. Louwen, J. G. Noltes, A. L. Spek, H. J. C. Ubbels, *J. Am. Chem. Soc.* **1982**, *104*, 6609–6616; f) J. Terheijden, G. van Koten, J. L. de Booys, H. J. C. Ubbels, C. H. Stam, *Organometallics* **1983**, *2*, 1882–1883.
[17] M. Panda, S. Das, G. Mostafa, A. Castiñeiras, S. Goswami, *Dalton Trans.* **2005**, 1249–1255.
[18] a) P. M. Maitlis, A. Haynes, B. R. James, M. Catellani, G. P. Chiusoli, *Dalton Trans.* **2004**, 3409–3419.
[19] a) D. N. Neogi, P. Das, A. N. Biswas, P. Bandyopadhyay, *Polyhedron* **2006**, *25*, 2149–2152; b) D. N. Neogi, A. N. Biswas, P. Das, R. Bhawmick, P. Bandyopadhyay, *Inorg. Chim. Acta* **2007**, *360*, 2181–2186.
[20] a) R. G. Parr, W. Yang, *J. Am. Chem. Soc.* **1984**, *106*, 4049–4050; b) F. Méndez, J. L. Gázquez, *J. Am. Chem. Soc.* **1994**, *116*, 9298–9301.
[21] a) H. C. Clark, L. E. Manzer, *J. Organomet. Chem.* **1973**, *59*, 411–428; b) B. Crociani, M. Nicolini, R. L. Richards, *Inorg. Chim. Acta* **1975**, *12*, 53–59; c) R. Usón, J. Forniés, P. Espinet, *J. Organomet. Chem.* **1976**, *116*, 353–359.
[22] a) J. Forniés, C. Fortuño, M. A. Gómez, B. Menjón, E. Herdtweck, *Organometallics* **1993**, *12*, 4368–4375; b) A. J. Canty, R. T. Honeyman, B. W. Skelton, A. H. White, *J. Organomet. Chem.* **1992**, *424*, 381–390; c) A. J. Canty, R. T. Honeyman, B. W. Skelton, A. H. White, *J. Organomet. Chem.* **1990**, *396*, 105–113; d) H. C. Clark, G. Ferguson, V. K. Jain, M. Parvez, *Organometallics* **1983**, *2*, 806–810; e) S. Chattopadhyay, C. Sinha, P. Basu, A. Chakravorty, *Organometallics* **1991**, *10*, 1135–1139; f) S. Chattopadhyay, C. Sinha, P. Basu, A. Chakravorty, *J. Organomet. Chem.* **1991**, *414*, 421–431.
[23] J. C. Muijsers, J. W. Niemantsverdriet, I. C. M. Wehman-Ooyevaar, D. M. Grove, G. van Koten, *Inorg. Chem.* **1992**, *31*, 2655–2658.
[24] F. M. Bickelhaupt, E. J. Baerends, W. Ravenek, *Inorg. Chem.* **1990**, *29*, 350–354.
[25] P. R. Ellis, J. M. Pearson, A. Haynes, H. Adams, N. Bailey, P. M. Maitlis, *Organometallics* **1994**, *13*, 3215–3226.
[26] a) L. M. Rendina, R. J. Puddephatt, *Chem. Rev.* **1997**, *97*, 1735–1754; b) J. K. Jawad, R. J. Puddephatt, *J. Chem. Soc., Dalton Trans.* **1977**, 1466–1469; c) J. K. Jawad, R. J. Puddephatt, *J. Organomet. Chem.* **1976**, *117*, 297–302.
[27] G. Ferguson, P. K. Monaghan, M. Parvez, R. J. Puddephatt, *Organometallics* **1985**, *4*, 1669–1674.
[28] V. D. Felice, B. Glovannitti, A. D. Renzi, D. Tesauro, A. Penunzi, *J. Organomet. Chem.* **2000**, *593–594*, 445–453.
[29] a) A. Yahav, I. Goldberg, A. Vigalok, *J. Am. Chem. Soc.* **2006**, *128*, 8710–8711; b) R. J. Puddephatt, J. D. Scot, *Organometallics* **1985**, *4*, 1221–1223.
[30] S. Dutta, S. M. Peng, S. Bhattacharya, *J. Chem. Soc., Dalton Trans.* **2000**, 4623–4627.
[31] M. Ghedini, D. Pucci, A. Crispini, G. Barberio, *Organometallics* **1999**, *18*, 2116–2124.
[32] B. S. Furniss, A. J. Hannaford, V. Rogers, P. W. G. Smith, A. R. Tatchell (Eds.), *Vogel's Text Book of Practical Organic Chemistry*, ELBS and Longman Group Ltd., London, **1978**, 4th ed..
[33] G. M. Sheldrick, *SHELX97*, University of Göttingen, Germany, **1997**.
[34] L. J. Farrugia, *WinGX Version 1.64, An Integrated System of Windows Programs for the Solution, Refinement and Analysis of Single-Crystal X-ray Diffraction Data*, Department of Chemistry, University of Glasgow, **2003**.
[35] PLATON: A. L. Spek, *J. Appl. Crystallogr.* **2003**, *36*, 7–13.
[36] L. J. Farrugia, *J. Appl. Crystallogr.* **1997**, *30*, 565–566.
[37] The ADF program system was obtained from Scientific Computing and Modeling, Amsterdam (http://www.scm.com/). For a description of the methods used in ADF, see: G. T. Velde, F. M. Bickelhaupt, E. J. Baerends, C. F. Guerra, S. J. A. Van Gisbergen, J. G. Snijders, T. Ziegler, *J. Comput. Chem.* **2001**, *22*, 931–967.
[38] S. H. Vosco, L. Wilk, M. Nusair, *Can. J. Phys.* **1980**, *58*, 1200–1211.
[39] A. D. Becke, *Phys. Rev. A* **1988**, *38*, 3098–3100.
[40] J. P. Perdew, Y. Wang, *Phys. Rev. B* **1992**, *45*, 13244–13249.
[41] a) A. Klamt, G. J. Schüürmann, *J. Chem. Soc. Perkin Trans. 2* **1993**, 799–805; b) A. Klamt, V. Jonas, *J. Chem. Phys.* **1996**, *105*, 9972–9981.
[42] S. Huzinaga, *J. Chem. Phys.* **1965**, *42*, 1293–1302.

Received: May 3, 2011
Published Online: August 5, 2011

